AIAA JOURNAL
Vol. 35, No. 2, February 1997

Trailing Vortex Wake Growth Characteristics of a High Aspect Ratio Rectangular Airfoil

Jamey Jacob,* Ömer Savaş,† and Dorian Liepmann‡
University of California, Berkeley, Berkeley, California 94720-1740

The growth characteristics of trailing vortex wakes are investigated in a towing tank. The wakes from a lifting rectangular NACA 0012 airfoil with an aspect ratio of 8 are studied up to 1400 chords downstream. The circulation Reynolds number ranged from 4×10^3 to 4×10^4. Digital particle image velocimetry is used to measure the velocity field in the cross-stream plane from which vorticity is calculated. The vortex pair is observed to be very stable and long-lived, showing little decay in the circulation of the individual vortices. The vorticity, however, diffuses over time within the cores of the vortices. This growth is found to be reminiscent of laminar diffusion. No Crow instabilities are observed within the range of these measurements.

Nomenclature

AR	= aspect ratio, $b/c = 8$
b	= airfoil span, 30 cm
c	= airfoil chord, 3.8 cm
c_l	= lift coefficient
L	= airfoil lift
Re_c	= chord Reynolds number, Uc/ν
Re_Γ	= vortex Reynolds number, Γ/ν
r_c	= vortex core radius
$r*$	= nondimensional core radius, $(r_c\, Re_c^{1/2}/c)$
s	= vortex separation distance
t	= time
U	= airfoil velocity, 50–160 cm/s
$\boldsymbol{u}$	= cross-stream velocity vector, normal to airfoil motion, $\boldsymbol{u}[y, z; x(t)] = \boldsymbol{u}(u, v)$
V	= downwash velocity
$\mathcal{V}$	= reduced downwash, Vb/Γ
x	= streamwise coordinate
y, z	= cross-stream coordinates
α	= angle of attack, −12 to +12 deg
Γ	= circulation, measured
Γ_0	= circulation, theoretical
ν	= kinematic viscosity, 0.01 cm²/s
ρ	= fluid density, 1 g/cm³
σ	= vortex core growth rate
τ	= nondimensional time, $tU/c = x/c$
ω	= vorticity in y–z plane

I. Introduction

THE trailing vortex wake is of equal interest to fluid dynamicists and air traffic administrators. This interest has been high since the inception of large air transport as shown by the contents of several review articles and symposium proceedings as well as a recent bibliography of vortex research done over the last 70 years.[1–7] This interest has grown after the wake vortices have been partially identified as the cause of some recent aircraft accidents.[8,9] This renewed interest can also be accredited to the development of powerful new experimental and numerical research tools. We use here digital particle image velocimetry (DPIV)[10] in the measurement of vortex wake flowfields.

Structural data on the far-field wake vortices are sparse. Full-scale measurements are often made by tower flyby techniques or ground anemometers[11–13] where ground effects and tower interference further complicate the flow. Despite their limitations, ground-based systems are being used as vortex tracking systems, which may be employed as a warning mechanism at airports.[12,14] Detailed measurements of the near-field vortex wake have recently been made using particle displacement velocimetry, laser Doppler velocimetry (LDV), and hot wire anemometry.[15–18] These have yielded important information on the initial roll-up process of the vortices but are nominally limited to measurements a few chords downstream of the airfoil. Recent measurements of the wakes of aircraft models and their effects on following wings have been made in the 80×120 foot wind tunnel at NASA Ames Research Center.[19] Results indicate that angle of attack has a large effect on the intensity of the vortex and the induced rolling moment on following aircraft, though the effects are not entirely predictable. Previous experiments of wings at large downstream distances have been conducted in water tunnels using other experimental methods. Using LDV, Ciffone and Orloff[20] found two characteristic regions in the wake, the first with little or no decay and the second where the maximum azimuthal velocity decayed inversely proportional to the square root of downstream distance, $(x/c)^{-1/2}$, which agrees with previous conclusions.[21] Another study in a water tank with a hydrogen bubble technique surmised that the rate of vortex decay was largely dependent upon the level of turbulence introduced into the system through the effects of Reynolds number and angle of attack.[22] As the measured decay rates were proportional to $(x/c)^{-7/8}$, it was cautioned that due to the low Reynolds number, the rate of decay measured would not correctly predict that of full-scale aircraft, though results from Iverson might indicate otherwise.[23]

Measurement of vorticity distribution in the vortex wake is essential in determining the stability characteristics of the wake, thus allowing further exploration of wake modification by artificial means. Extraction of this information requires instantaneous field measurements, whereas most of the previously cited research consists of point-based measurements, which suffer from vortex wandering.[18,24] DPIV offers planar, instantaneous, continuous data acquisition. Since DPIV allows determination of an instantaneous velocity field at a single slice of the three-dimensional vortex motion, temporal changes in the field can be measured by fixing the slice relative to the airfoil, whereas spatial changes can be measured by fixing the slice relative to a stationary observer. Preliminary results have been presented earlier.[25]

The purpose of this study is to produce sufficient data for general statements to be made about the long-term evolution of the vortex wake. In particular, our interest lies in wings with high aspect ratios

Presented as Paper 95-1841 at the AIAA 13th Applied Aerodynamics Conference, San Diego, CA, June 19–22, 1995; received Oct. 31, 1995; revision received Aug. 21, 1996; accepted for publication Oct. 18, 1996; also published in *AIAA Journal on Disc*, Volume 2, Number 2.

*Visiting Postdoctoral Fellow, Department of Mechanical Engineering; currently Assistant Professor, Department of Mechanical Engineering, University of Kentucky, Lexington, KY 40506-0108. Member AIAA.

†Associate Professor, Department of Mechanical Engineering. Associate Fellow AIAA.

‡Assistant Professor, Department of Mechanical Engineering.

similar to those currently used in the commercial aviation industry, where the appearance of Crow rings is delayed due to the greater spacing between vortex cores. In this context, it is important that the downstream vortical structure of the wake be determined. It is then possible to examine the most probable modes of instabilities in the vortices. Excitation of these instabilities by passive or active methods then may become a realizable goal.

II. Experimental Procedure

A. Experimental Facilities

The experiments are conducted in the Naval Architecture and Offshore Engineering Towing Tank of the University of California at Berkeley. The arrangement is shown in Fig. 1. The tank is approximately 70 m long, 2.4 m wide, and 1.7 m deep. Water depth is about 1.5 m. A towing carriage moves along rails above the tank at speeds from $U = 10$ to 160 cm/s with an accuracy of better than 1%. The tank has a 3-m-long glass viewing station near the center where the current measurements are done.

The wing configuration and the coordinate system are shown in Fig. 2. The airfoil is a rectangular planform with a NACA 0012 cross section. The wing span b is 30 cm, and the chord c is 3.8 cm with an aspect ratio AR of 8. The airfoil was constructed of stainless steel. The endcaps are NACA 0012 elliptical contours with a 2:1 ratio constructed of brass. The strut, located at midspan, is a NACA 0010 airfoil of the same construction and a larger hollow streamlined strut that is fastened to the carriage. All wetted junctions are faired. The angle of attack α of the airfoil is variable from -12 to $+12$ deg in 2-deg increments.

A light sheet is generated in the tank using a 10-W argon-ion laser and a 200 μm multimode fiber-optical cable. Total losses are estimated to be about 50%. The light sheet is projected from the bottom of the tank using a 6-mm glass rod to focus the beam into a light sheet. The light sheet is about 1 cm thick. The region upstream of the sheet is locally seeded with 300–600 μm styrene-butadiene polymer spheres with a specific gravity of approximately 1.05, though the particles, being porous, are slightly buoyant. A noninterlaced charge-coupled device (CCD) camera is used to record the flowfield at an oblique angle of approximately 57 deg to the viewing window, or approximately 39 deg to the light sheet as measured

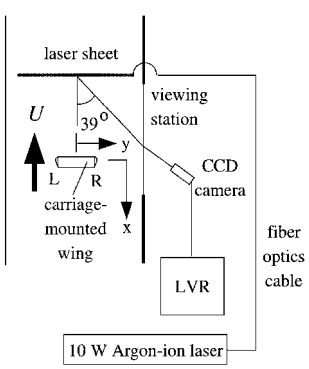

Fig. 1 Experimental arrangement of tow tank and imaging system.

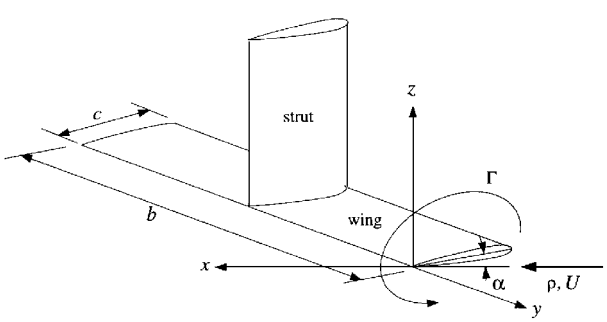

Fig. 2 Wing coordinate system; x is the streamwise coordinate and y–z is the cross-stream plane. The wing is at angle of attack α to the freestream velocity U. The wing is a NACA 0012 rectangular plan form with 2:1 elliptical contours at the wing tips. The span b = 30 cm and chord c = 3.8 cm.

from the airfoil velocity vector. Flow images are recorded on a laser video recorder (LVR) at 30 Hz and are later digitized for processing at 512×480 pixels resolution.

B. Data Processing

Instantaneous planar velocity fields $\boldsymbol{u} = \{u[y, z; x(t)], v[y, z; x(t)]\}$ are determined from sequential images using a DPIV algorithm[26] based on that developed by Willert and Gharib.[27] The method uses a new iterative technique to improve valid data density in sparsely seeded regions. For the runs in this study, an interrogation region of 16×16 pixels is used with 75% overlap. Velocity vector fields are determined from image pairs taken $\frac{1}{30}$ second apart. Once the velocity vectors are determined, the fields are corrected for the image distortion. A local median filtering technique is used to remove most of the bad vectors.

The streamwise vorticity component ω is determined from an estimate of the circulation Γ about the smallest path on the velocity grid around a point

$$\Gamma = \oint \boldsymbol{u} \cdot d\boldsymbol{l} \tag{1}$$

Then Stokes' theorem gives

$$\omega = \Gamma / dA \tag{2}$$

where dA is the area bounded by the contour of integration in Eq. (1). This is essentially a differentiation of the velocity data. Although this method tends to give lower values for peak vorticity, it does minimize the error introduced by spurious vectors. The domain of the vorticity field is smaller than that of the velocity field by an amount imposed by the size of the integration contour in Eq. (1). The circulation Γ of each vortex is calculated using Eq. (1) along a rectangular path around the vortex. The paths for the left and right vortices have one side in common along the centerline of the vortex pair, and the remaining sides are near the edges of the data plane.

The measurements suffer from a spatial distortion due to the oblique observation angle and the finite thickness of the light sheet. This problem is more pronounced in the v component of the velocity vector. Because of the oblique viewing angle and the thick light sheet, there is the possibility of the cross-stream velocity measurements being contaminated by the streamwise velocity component. Visually following particles, however, reveals that the motion is primarily two dimensional and particles tend to remain in the laser sheet for several seconds. Thus, the measurements should represent the flow well. Based on these visual observations, there exist axial velocities in the vortex cores that are estimated to be on the order of the wing velocity in the immediate vicinity of the wing, though relative motion cannot be determined by visual inspection alone. The buoyant motion of the particles is negligible compared with the motion in the vortex wake as shown by the maximum relative tracking error estimated at < 2% (Ref. 28). Because of the density difference between the particles and water, however, errors due to centrifugal forces are incurred. These are most significant near the vortex cores, thus manifesting themselves as errors in the vorticity estimates in regions of highly curved pathlines. As noted earlier, circulation is calculated along a path well outside of the vortex cores to circumvent this difficulty. The spatial resolution of vorticity is less than that of velocity due to the method of calculation. To test the accuracy of the DPIV algorithm for this study, false data are generated with two opposite signed Rankine vortices of approximate size, location, and strength expected in the tow tank tests. Seeding is matched by using Gaussian particles of the same number, intensity, and pixel size as those recorded during the measurements. Comparisons with the given velocity field show errors of approximately 5% for velocities with the error being highest near the vortex cores. The vortex radii are estimated to within 10% with the error increasing as the cores become smaller. To determine the core size, slices are taken at several different angles across the vortex cores, and the resulting profiles are splined to help minimize discretization. The radius is then determined by the average distance of maximum azimuthal velocity from the peak vorticity.

III. Results

A total of 54 runs are done with velocities ranging from $U = 50$ to 160 cm/s and angles of attack α from -12 to $+12$ deg, giving a range of chord based Reynolds number $Re_c = cU/\nu$ from 2×10^4 to 6×10^4. The data runs discussed in this paper are shown in Table 1. The longest run is approximately 2000 chords (250 spans) downstream of the observation station, though the nominal measurements are done from 200 to 1400 chords (25–175 spans) downstream. As the vortex downwash is proportional to the airfoil speed and angle of attack, longer data sets are obtained for parameters with low U and α, because higher values produce vortices that travel out of the viewing region more quickly or interact with the free surface or the bottom of the tank. The percentage of valid data, as determined from a threshold comparison of vectors, ranged between 75 and 98%. Good data are generally data sets with a valid data rate of 95% or higher. This limited the number of usable sets without excessive postprocessing. Because of the high angle of attack of runs 7–9, we expect the flows to be separated.

The circulation based Reynolds number, $Re_\Gamma = \Gamma/\nu$, is the appropriate parameter for the vortex wake. A theoretical circulation Γ_0, a surrogate for the actual vortex circulation Γ, is estimated from the Kutta–Joukowsky theorem. Treating the wing as a segment of an infinite lifting line, the relationship between lift L and circulation Γ_0 is given by

$$L = \rho b U \Gamma_0 \tag{3}$$

The lift L may be written in terms of the lift coefficient c_l as $L = c_l \rho U^2 bc/2$. Equation (3) results in

$$\Gamma_0 = \tfrac{1}{2} c_l c U \tag{4}$$

Again, by using an infinite planar wing, $c_l = 2\pi\alpha$. This gives

$$\Gamma_0 = \pi \alpha c U \tag{5}$$

hence

$$Re_{\Gamma_0} = \pi \alpha Re_c \tag{6}$$

Thus, the circulation Reynolds number Γ_0/ν ranged up to 4×10^4. Values for both Re_c and Re_{Γ_0} are shown in Table 1.

Using the assumption of viscous diffusion, the vortex core radius r_c is scaled as $r_c Re_c^{1/2}/c$ whose dependence on the age of the vortex is calculated by Moore and Saffman[29] as

$$r* = \frac{r_c Re_c^{\frac{1}{2}}}{c} = 2.92\left(\frac{x}{c}\right)^{\frac{1}{2}} \tag{7}$$

Velocity and vorticity are scaled by U and c/U, respectively, and the characteristic time scale is given by

$$\tau = tU/c = x/c \tag{8}$$

As an example, data for run 5 are shown in Figs. 3–5 with parameters $U = 100$ cm/s and $\alpha = -8$ deg. Examples of corrected vorticity fields are shown in Fig. 3. The contours are at 1 s^{-1} intervals. In the first of these figures, the wing has just passed through the laser sheet ($x/c \approx 5$), and the wake generated by the strut/wing connection can clearly be seen between the two vortices. This wake decays quite rapidly and does not appear to affect the evolution of

Table 1 Experimental parameters of the runs used in this study

Run no.	U, m/s	α, deg	Re_c, $\times 10^{-4}$	Re_{Γ_0}, $\times 10^{-4}$	z_{max}, z/c
1	0.5	−4	2.0	0.42	450
2	1.0	−4	4.0	0.84	900
3	1.5	−4	6.0	1.25	1350
4	0.5	−8	2.0	0.84	450
5	1.0	−8	4.0	1.67	900
6	1.5	−8	6.0	2.51	1350
7	0.5	−12	2.0	1.25	450
8	1.0	−12	4.0	2.50	900
9	1.5	−12	6.0	3.74	1350

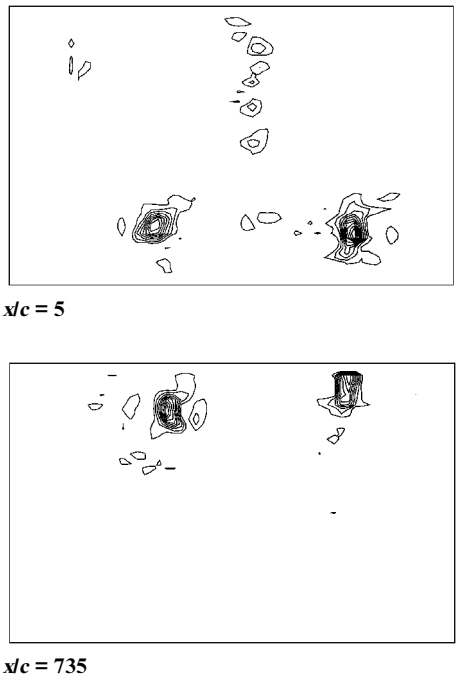

Fig. 3 Equispaced absolute isovorticity contours for run 5 (Table 1). The vortex pair moved up due to negative angle of attack.

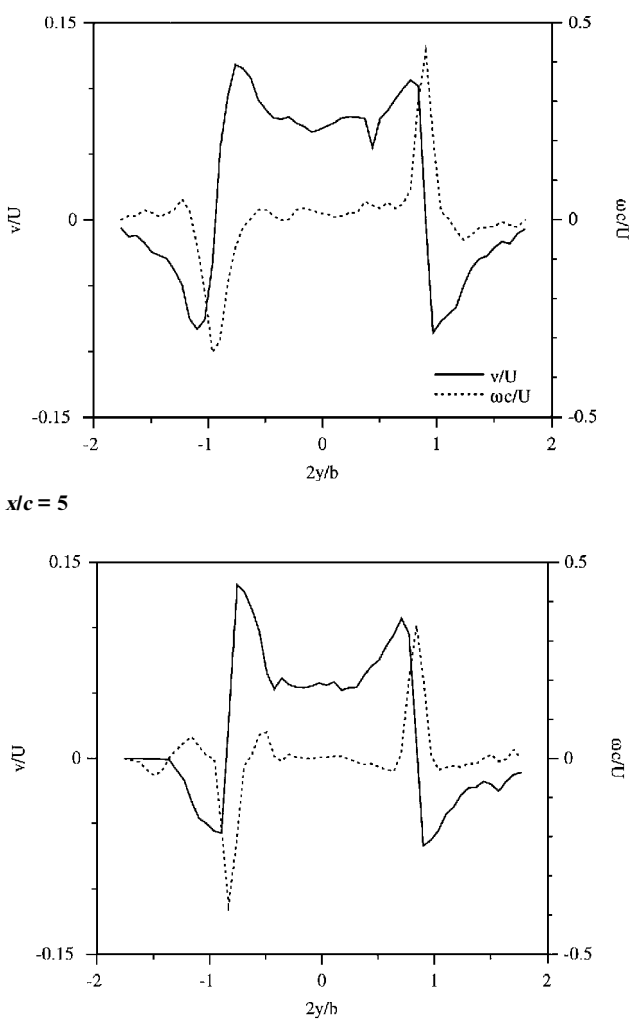

Fig. 4 Velocity (solid line) and vorticity (dashed line) profiles along vortex pair centerline for run 5 (Fig. 3).

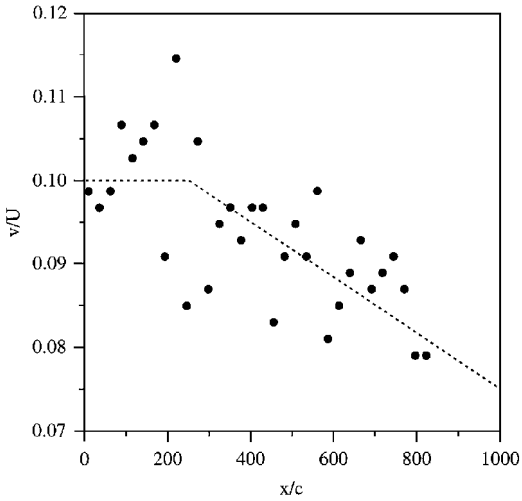

Fig. 5 Maximum tangential velocity history for run 5.

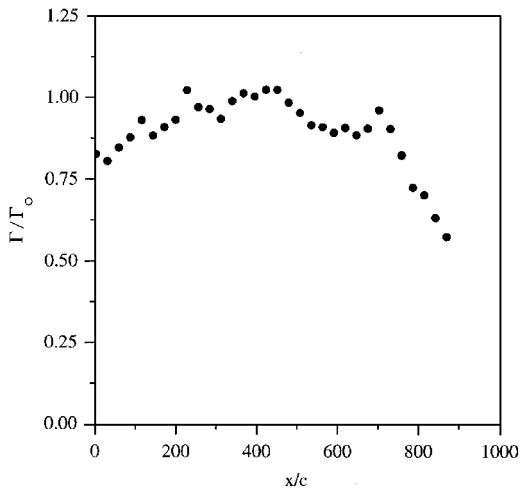

Fig. 6 Circulation history for run 5.

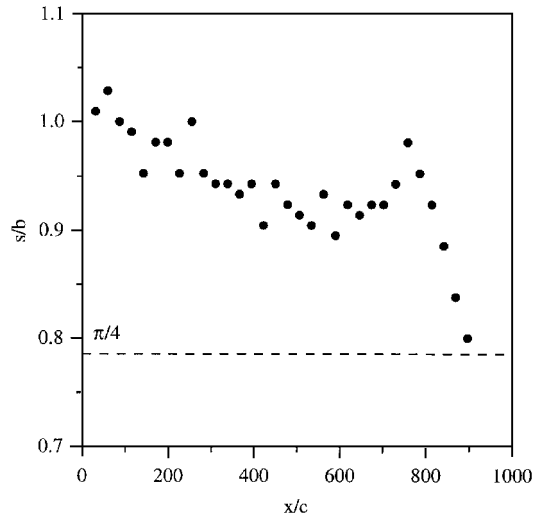

Fig. 7 Vortex core separation distance history for run 5. The dashed line indicates $\pi/4$ expected for an elliptically loaded wing.

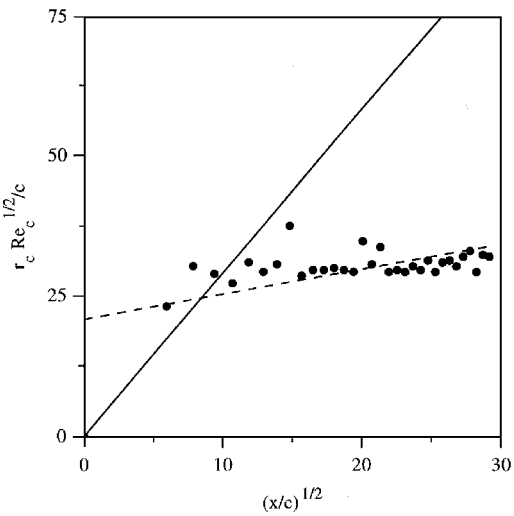

Fig. 8 Nondimensional radii history for run 5. The solid line is the prediction from Moore and Saffman.[29] The dashed line is the curvefit used to determine the growth rate.

the wake. The vortices are moving upward under their own motion due to the negative angle of attack of the wing. The downstream data are at $x/c \approx 735$. The fingering at the vortex corners is due to DPIV biasing. Corresponding profiles of velocity and vorticity along the vortex centerlines (Fig. 4) illustrate the very slow growth of the vortices. The vortices have moved slightly closer to each other. Nondimensional maximum tangential velocity is shown in Fig. 5. The velocities from both vortices are averaged. The data show little variation initially followed by a region of decay, as shown in previous studies.[20] This variation is due to spreading of vorticity in the core rather than an overall decay of the wake. The average circulation of the left and right vortices is shown in Fig. 6. Both vortices exhibit the same behavior. There is a slight fluctuation in the circulation, possibly due to the vortex completing the roll-up process, and then a sharp decay as the vortex wake moves across the image region. Figure 7 shows the separation distance between the vortex cores. The separation gradually approaches the theoretical value of $\pi/4$ for elliptically loaded wings. The fluctuations at high values of x/c are possibly due to the vortices approaching the free surface where they tend to separate laterally with their respective image vortices. This could also be evidence of the onset of the Crow instability, however.

Nondimensionalized average vortex radii are shown in Fig. 8. In examining this example, it must be noted that the radii are instantaneous snapshots of the vortex core. Thus, the radii shown here reveal large (and discrete) fluctuations in the core size, which are confirmed by flow visualization. The measurements are taken over a wide range of the axial distance (x/c). Near-wake measurements are not as accurate as those farther downstream, due to tighter streamline curvatures in the flow. Equation (7) from Moore and Saffman[29] for laminar flow is shown in Fig. 8 as a solid line. The data show slower growth than that predicted by the theory.

IV. Discussion

A. Vortex Wake Motion

The vortex pair is characterized by its strength and the separation. The speed at which the pair translates is

$$V = \Gamma/2\pi b \tag{9}$$

where the vortex separation is taken to be nominally the wing span b. Actual vortex separation s is somewhat smaller than b. Using arguments similar to those leading to Eq. 5, the relation between the V and U becomes

$$V \propto c_l(c/b)U \tag{10}$$

For a symmetric airfoil $c_l \propto \alpha$, hence the reduced downwash velocity

$$\forall \neq Vb/\Gamma \tag{11}$$

where $\forall$ is expected to be constant far downstream. Equation (9) implies a reduced downwash of $\forall \neq \frac{1}{2}\pi$. This definition may be

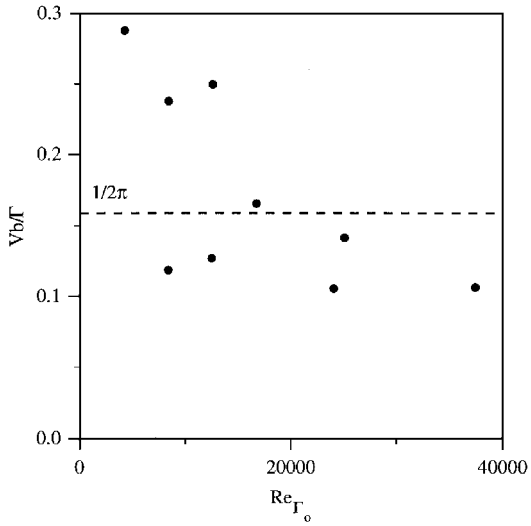

Fig. 9 Measured values of reduced downwash $\gamma = Vb/\Gamma$. The dashed line indicates $\frac{1}{2}\pi$ expected for a pair of line vortices.

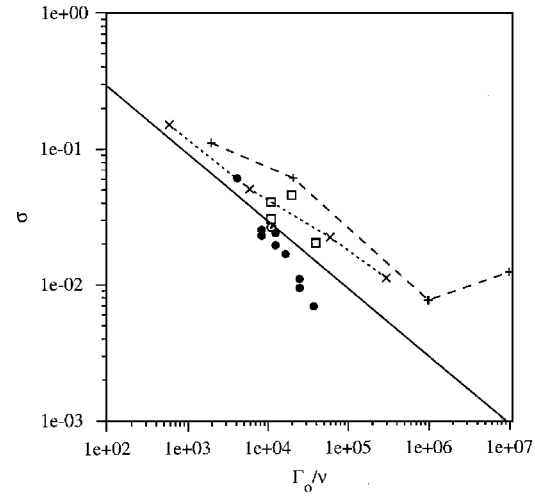

Fig. 10 Core growth rate σ vs vortex Reynolds number Γ_0/ν for experiments here and elsewhere: ●, this study, runs 1–9; ⊙, wind-tunnel run from Jacob et al.[33]; □, Baker et al.[24]; +, Govindaraju and Saffman[32]; ×, Zeman's Reynold's stress closure model[31]; and solid line, prediction for viscous vortex from Moore and Saffman.[29]

looked on as a check on the self-consistency of the data by comparing the independent measurements of the downwash velocity V and the circulation Γ. The measured reduced downwash velocities are shown in Fig. 9. Note that the measured circulation Γ is used in scaling V. The data are scattered around the expected constant value of $\frac{1}{2}\pi$. This scatter is due largely to differences in measured and predicted values of the circulation. The agreement between the prediction and the measurements is, nevertheless, acceptable.

B. Vortex Wake Longevity

Much of the interest in trailing vortex wakes lies in their decay. Previous studies have had some success in determining empirical relations of vortex decay,[11,13,22] but no method has yet been found to accurately predict decay in vortex wakes outside of the laboratory. This is due in part to the complications from outside influences, such as background shear, turbulence, stratification, and the differences in vortex structure from varying wing configurations. There is disagreement as to the mechanism of the decay process. When left to their own devices, the vortex pair should decay mainly through viscous dissipation in the absence of detrainment. The amount of this dissipation is in question. Figure 5 shows a gradual decay in peak velocity for run 5. As mentioned earlier, this decay is the result of a redistribution of vorticity rather than a loss in total circulation of the vortex. Figure 6 corroborates this claim where circulation remains nearly constant.

Crow[30] gives the time scale for the onset of the Crow instability to be the inverse of the rate of amplification,

$$a^{-1} = 9.4(AR/c_l)(s/U) \tag{12}$$

For the largest value of U used here, this gives $a^{-1} = 13$ s. The entire measurement period is just over 30 s, indicating that if the Crow instability were to form, it would still be in the early stages and might not be recognized as such.

C. Vortex Core Growth Rate

A laminar vortex grows by viscous diffusion. At high Reynolds numbers, however, turbulence must be considered though its precise role in vortex dynamics is unclear. There is ample evidence that trailing vortices at high Reynolds numbers grow slowly and persist for inordinately long times. Figure 10 compares numerous findings on the growth rate of the vortices as a function of the vortex Reynolds number Γ/ν. The growth rate, the rate of change of the radius where the azimuthal velocity is at its maximum, is defined as

$$\sigma = \frac{\Delta r_c}{\Delta(\Gamma_0 t)^{\frac{1}{2}}} = \frac{\Delta r*}{\Delta(x/c)^{\frac{1}{2}}}\left(\frac{\Gamma_0}{\nu}\right)^{-\frac{1}{2}} \tag{13}$$

following Zeman.[31] The experimental points consist of those by Baker et al.,[24] those compiled by Govindaraju and Saffman,[32] and the current ones, including a recent wind-tunnel case.[33] The current results are extracted from vortex size histories as that shown in Fig. 8, where it is assumed that $r_c = 0$ at $x/c = 0$. The growth rate of a viscous vortex core determined by the analysis of Moore and Saffman,[29] $2.92(\Gamma/\nu)^{-1/2}$, is also shown. The experimental data very strongly suggest a viscous behavior of the vortex. In view of this close agreement, Moore and Saffman's analytic result may be considered a good prediction of the vortex growth rate in the wake of a lifting body when the interaction between the vortices has not developed yet. The results from Devenport et al.[18] are not shown in Fig. 10 because the values tabulated in their work show no growth for $x/c \lesssim 30$. It is not clear whether this can be attributed to vortex wandering or the limited range of the measurements. Zeman's[31] calculations, which are shown in Fig. 10, indicate that when turbulence is modeled by a Reynolds stress closure model, the growth rate is determined by the molecular viscosity. Thus the vortex core size should grow as $(\nu t)^{1/2}$ where t is the age of the vortex. Zeman's main conclusion is that turbulence is only secondary to the longevity of the vortices. He based this conclusion on a comparison in his Fig. 2 of his numerical results with some experimental data where the measurements from Baker et al.[24] are misplaced. That Zeman's Reynolds stress closure model gives a similar behavior may be interpreted either as a confirmation of this result if the modeling is assumed to be indisputable, which is unlikely, or a confirmation of the suitability of the modeling for this particular case, which is more likely. Zeman finds that results based on k-ϵ turbulence models are poor.

V. Summary

The trailing vortex wake of a rectangular NACA 0012 airfoil with $AR = 8$ is investigated. The wake is mapped using DPIV up to 1400 chords (175 spans) downstream. The chord Reynolds number ranged from 2×10^4 to 6×10^4 and the circulation Reynolds number from 4×10^3 to 4×10^4. This measurement technique gives continuous instantaneous planar velocity fields. This capability eliminates problems associated with vortex wandering when mapping the flowfield with a single point probe such as a laser Doppler velocimeter or a hot-wire anemometer. The planar velocity vector fields are used to determine the vorticity field in the vortex wake. The results show that, for these moderate Reynolds numbers at this high aspect ratio, the vortices are very stable and show little growth within the range of these measurements. This is reminiscent of viscous growth. The influence of the vortices upon each other is minimal. No Crow instabilities are observed in these experiments.

Acknowledgments

This work was supported in part by California Department of Transportation Grant RTA 65V749. We benefited from discussions with P. Marcus, D. Fabris, and T. Matsushima of the University of California, Berkeley. We would also like to thank R. Yeung at the University's Naval Architecture and Offshore Engineering Department.

References

[1]Widnall, S. E., "The Structure and Dynamics of Vortex Filaments," *Annual Review of Fluid Mechanics*, Vol. 27, 1974, pp. 141–165.

[2]Hall, M. G., "Vortex Breakdown," *Annual Review of Fluid Mechanics*, Vol. 4, 1972, pp. 775–802.

[3]Smith, J. H. B., "Vortex Flows in Aerodynamics," *Annual Review of Fluid Mechanics*, Vol. 18, 1986, pp. 221–242.

[4]Olsen, J. H., Goldburg, A., and Rogers, M. (eds.), *Aircraft Wake Turbulence and Its Detection*, Plenum, New York, 1971.

[5]Gessow, A. (ed.), *Symposium on Wake Vortex Minimization*, NASA SP-4096, Feb. 1976.

[6]Hallock, J. N., "Aircraft Wake Vortices: An Assessment of the Current Situation," U.S. Dept. of Transportation, DOT-FAA-RD-90-20, DOT-VNTSC-FAA-90-6, John A. Volpe National Transportation Systems Center, Cambridge, MA, Jan. 1991.

[7]Hallock, J. N., "Aircraft Wake Vortices: An Annotated Bibliography (1923-1990)," U.S. Dept. of Transportation, DOT-FAA-RD-90-30, DOT-VNTSC-FAA-90-7, John A. Volpe National Transportation Systems Center, Cambridge, MA, Jan. 1991.

[8]Nordwall, B. D., "Wake Turbulence Tests to Determine Safe Separation," *Aviation Week and Space Technology*, Nov. 1994, p. 85.

[9]Phillips, E. H., "Vortex Tests May Yield Clues to USAir Crash," *Aviation Week and Space Technology*, Oct. 1995, p. 33.

[10]Cho, Y.-C., "Digital Image Velocimetry," *Applied Optics*, Vol. 28, No. 4, 1989, pp. 740–748.

[11]Garodz, L., and Clawson, K., "Vortex Wake Characteristics of B757-200 and B767-200 the Tower Fly-By Technique," NOAA-TM-ERL-ARL-199-V1, Jan. 1993.

[12]Kopp, F., "Doppler Lidar Investigation of Wake Vortex Transport Between Closely Space Parallel Runways," *AIAA Journal*, Vol. 32, No. 4, 1994, pp. 805–810.

[13]Teske, M. E., Bilanin, A. J., and Barry, J. W., "Decay of Aircraft Vortices Near the Ground," *AIAA Journal*, Vol. 31, No. 8, 1993, pp. 1531, 1532.

[14]Balser, M., McNary, C. A., and Nagy, A. E., "Acoustic Backscatter Radar System for Tracking Aircraft Trailing Vortices," *Journal of Aircraft*, Vol. 11, No. 9, 1974, pp. 556–562.

[15]Shekarriz, A., Fu, T. C., Katz, J., and Huang, T. T., "Near-Field Behavior of a Tip Vortex," *AIAA Journal*, Vol. 21, No. 1, 1991, pp. 112–118.

[16]Staufenbiel, R., and Vitting, T., "Formation of Tip Vortices and Vortex Wake Alleviation by Tip Devices," *Proceedings of the 17th ICAS Congress*, AIAA, Washington, DC, 1990, pp. 279–291.

[17]Szafruga, J., and Ramaprian, B. R., "LDA Measurements over the Tip Region of a Rectangular Wing," AIAA Paper 95-1780, June 1995.

[18]Devenport, W. J., Rife, M. C., Liapis, S. I., and Follin, G. J., "The Structure and Development of a Wing-Tip Vortex," *Journal of Fluid Mechanics*, Vol. 312, April 1996, pp. 67–106.

[19]Rossow, V. J., Fong, R. K., Wright, M. S., and Bisbee, L. S., "Vortex Wakes of Two Subsonic Transports as Measured in 80- by 120-Foot Wind Tunnel," AIAA Paper 95-1900, June 1995.

[20]Ciffone, D. L., and Orloff, K. L., "Axial Flow Measurements in Trailing Vortices," *AIAA Journal*, Vol. 12, No. 8, 1974, pp. 1154, 1155.

[21]McCormick, B. W., Tangler, J. L., and Sherrieb, H. E., "Structure of Trailing Vortices," *Journal of Aircraft*, Vol. 5, No. 3, 1968, pp. 260–267.

[22]Lezius, D. T., "Water Tank Study of the Decay of Trailing Vortices," *AIAA Journal*, Vol. 12, No. 8, 1974, pp. 769–779.

[23]Iverson, J. D., "Correlation of Turbulent Trailing Vortex Decay Data," *Journal of Aircraft*, Vol. 13, No. 5, 1976, pp. 338–342.

[24]Baker, G. R., Barker, S. J., Bofah, K. K., and Saffman, P. G., "Laser Anemometer Measurements of Trailing Vortices in Water," *Journal of Fluid Mechanics*, Vol. 65, Aug. 1974, pp. 325–336.

[25]Jacob, J. D., Liepmann, D., and Savaş, Ö., "Experimental Investigation of the Trailing Vortex Wake of a Rectangular Wing," AIAA Paper 95-1841, June 1995.

[26]Fabris, D., "Combined Experimental and Computational Investigation of a Vortex Ring Impinging Normally on a Wall," Ph.D. Dissertation, Dept. of Mechanical Engineering, Univ. of California, Berkeley, CA, May 1996.

[27]Willert, C. E., and Gharib, M., "Digital Particle Image Velocimetry," *Experiments in Fluids*, Vol. 10, Jan. 1991, pp. 181–193.

[28]Agui, J. C., and Jimenez, J., "On the Performance of Particle Tracking," *Journal of Fluid Mechanics*, Vol. 185, Dec. 1987, pp. 447–468.

[29]Moore, D. W., and Saffman, P. G., "Axial Flow in Laminar Trailing Vortices," *Proceedings of the Royal Society of London A*, Vol. 333, June 1973, pp. 491–508.

[30]Crow, S. C., "Stability Theory for a Pair of Trailing Vortices," *AIAA Journal*, Vol. 8, No. 12, 1970, pp. 2172–2179.

[31]Zeman, O., "The Persistance of Trailing Vortices: A Modeling Study," *Physics of Fluids*, Vol. 7, No. 1, 1995, pp. 135–143.

[32]Govindaraju, S. P., and Saffman, P. G., "Flow in a Turbulent Trailing Vortex," *Physics of Fluids*, Vol. 14, No. 10, 1971, pp. 2074–2080.

[33]Jacob, J. D., Savaş, Ö., and Liepmann, D., "Experimental Investigation of Forced Wake Vortices of a Rectangular Wing," AIAA Paper 96-2497, June 1996.